Deep magma storage at Hekla volcano, Iceland, revealed by InSAR time series analysis

Benedikt G. Ofeigsson,[1] Andrew Hooper,[2] Freysteinn Sigmundsson,[1] Erik Sturkell,[3] and Ronni Grapenthin[4]

Received 29 March 2010; revised 31 January 2011; accepted 14 February 2011; published 5 May 2011.

[1] Hekla volcano is one of the most active volcanoes in Iceland. The most recent eruption occurred from 26 February to 8 March 2000 when about 0.19 km^3 of magma was erupted. We present deformation data from multitemporal analyses of synthetic aperture radar (SAR) images acquired between 1993 and 2008, focusing on pixels with low-phase variance (using persistent scatterer and small baseline approaches). Prior to and after the 2000 eruption, we find a broad area of inflation around the volcano (radius about 20 km), with satellite line-of-sight (LOS) shortening of up to 5 mm/yr. We interpret this signal as the result of pressure increase in a deep-seated magma chamber, which we model as a spherical source at 14–20 km depth increasing in volume by 0.003–0.02 km^3/yr. Within a ~6 km radius of the summit of the volcano, a LOS lengthening is superimposed on the broad inflation signal, which correlates partly with recent lava flows. We interpret this signal as the result of thermally contracting lava flows, combined with viscoelastic yielding due to the load of the volcano and its lavas. Coeruptive deflation during the 2000 eruption was similar to the cumulative inflation from 1993 to 2000 and is consistent with a spherical magma chamber at 14–18 km depth that decreases in volume by 0.04–0.08 km^3. Interferograms spanning the 2000 eruption show a local coeruptive deformation signal near the eruptive fissure. This is consistent with a dike opening from the surface to depths up to 5.8 km with a volume of 0.005–0.006 km^3.

Citation: Ofeigsson, B. G., A. Hooper, F. Sigmundsson, E. Sturkell, and R. Grapenthin (2011), Deep magma storage at Hekla volcano, Iceland, revealed by InSAR time series analysis, *J. Geophys. Res.*, *116*, B05401, doi:10.1029/2010JB007576.

1. Introduction

[2] Iceland lies on the Mid-Atlantic Ridge, the divergent boundary between the North American and Eurasian plates. High magmatic activity and relatively dense volcano monitoring has allowed various studies of magmatic plumbing systems with geodetic techniques. At some of the more active volcanoes, including Grímsvötn, Katla, Krafla and Askja, shallow magma chambers have been identified at 2–5 km depth [*Sturkell et al.*, 2006a; *Sigmundsson*, 2006]. However, geodetic evidence also suggests deeper (≥10 km) deformation sources in a number of areas, giving an opportunity to study magma migration in the lower crust. The best documented case is a 2007–2008 magma intrusion into the lower crust east of Askja volcano, close to Mt. Upptyppingar, at 14–22 km depth [*Hooper et al.*, 2008]. A magma source north of Krafla has been suggested at about 21 km depth [*de Zeeuw-van Dalfsen et al.*, 2004], and beneath Bárdabunga at about 10 km depth [*Pagli et al.*, 2007]. *Sturkell et al.* [2006b] suggest a deep magma source at 16 km for Askja. At Hekla volcano, evidence of a deep magma source is inferred but depth estimates are uncertain due to complex and subtle deformation spread over a large area.

[3] In south Iceland, the plate boundary has two parallel volcanic zones: the Western Volcanic Zone (WVZ) and the Eastern Volcanic Zone (EVZ). These two branches of the plate boundary are connected by an E-W oriented transform, the South Iceland Seismic Zone (SISZ) [*Einarsson*, 1991]. Hekla volcano is located near the intersection of the EVZ and SISZ (Figure 1). It is one of Iceland's most active volcanoes with 18 summit eruptions during the last 1100 years. Until 1947, Hekla erupted 1–2 times every century, but since an eruption in 1970 Hekla has erupted approximately every 10 years, in 1980–1981, 1991 and 2000. The most recent eruption occurred from 26 February to 8 March 2000, when an estimated 0.19 km^3 (dense rock equivalent, DRE) was ejected [*Höskuldsson et al.*, 2007]. Most seismicity at Hekla occurs prior to and during eruptions. Numerous small earthquakes were associated with the onset of the 2000 eruption. The first earthquakes occurred approximately 80 min before

[1]Nordic Volcanological Center, Institute of Earth Sciences, University of Iceland, Reykjavík, Iceland.
[2]Delft Institute of Earth Observation and Space Systems, Delft University of Technology, Delft, Netherlands.
[3]Department of Earth Sciences, University of Gothenburg, Gothenburg, Sweden.
[4]Geophysical Institute, University of Alaska Fairbanks, Fairbanks, Alaska, USA.

0148-0227/11/2010JB007576

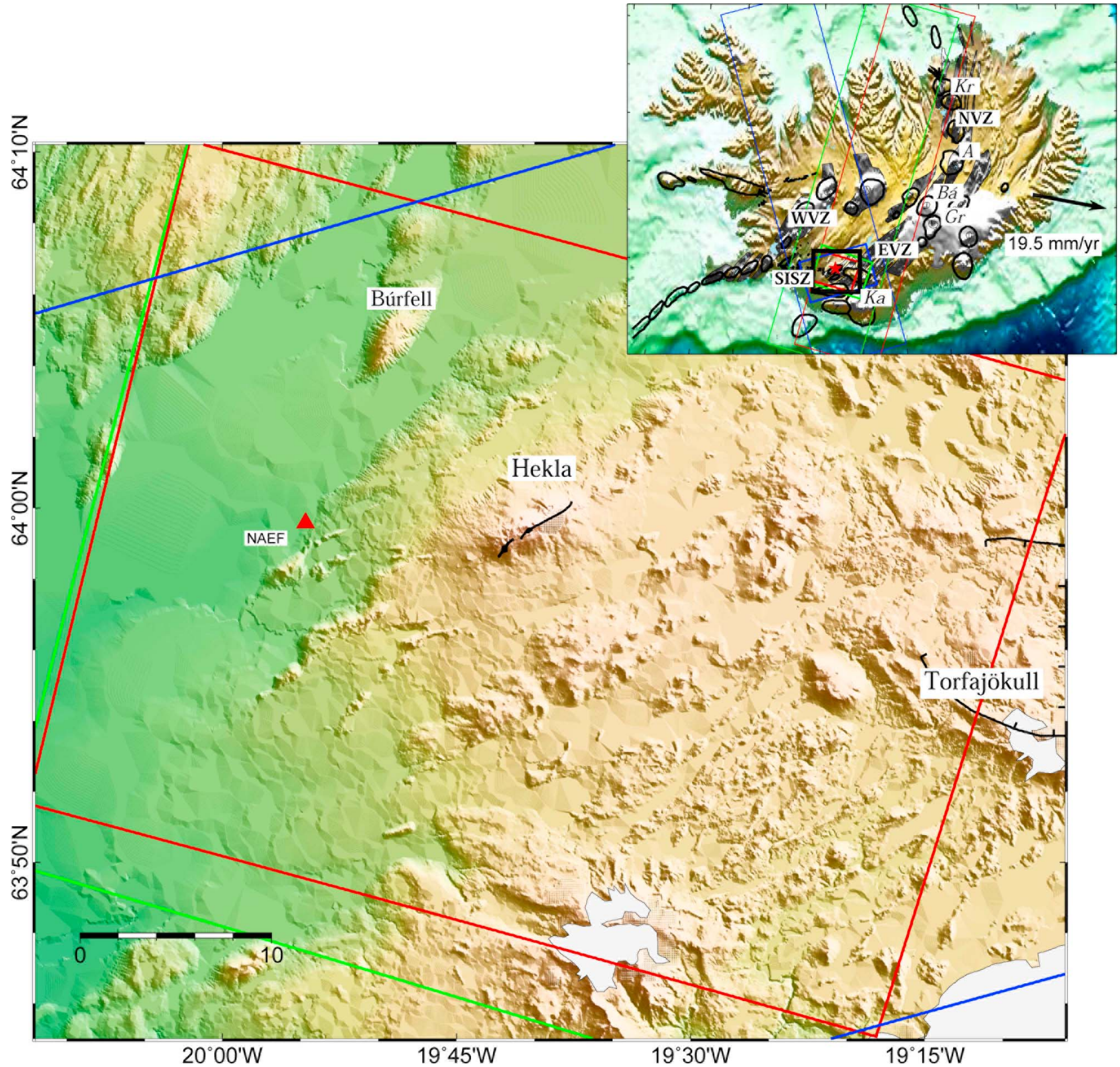

Figure 1. Hekla volcano and its surroundings in south Iceland. Hekla is an elongated ridge reaching an elevation of 1490 m. The black line along the summit indicates the 2000 eruptive fissure. The red triangle shows the optical leveling tilt station Næfurolt (NAEF) that has proven to be a long-term indicator of pressure in a magma source under Hekla. The map also shows the outline of Torfajökull caldera, an active central volcano east of Hekla. Inset shows the general tectonic setting of Iceland. Volcanic systems with central volcanoes (black oval outlines) and fissure swarms (gray areas) are located along the divergent plate boundary [*Einarsson and Sæmundsson*, 1987]. Black arrow shows the full spreading vector of 19.5 mm/yr in the direction indicated by the REVEL model [*Sella et al.*, 2002]. In the south the plate boundary divides up into the Western Volcanic Zone (WVZ) and the Eastern Volcanic Zone (EVZ). Hekla lies at the intersection of the EVZ and the South Iceland Seismic Zone (SISZ). The labeled volcanic systems are A, Askja; Bá, Bárdarbunga; Gr, Grímsvötn; ka, Katla; kr, Krafla. Red boxes indicate ERS track 52, blue boxes indicate ERS track 359, and green boxes indicate Envisat track 324.

the eruption and were shallow (≤3 km). Around 30 min before the eruption started, earthquakes with hypocenters from 6–14 km depth occurred. No propagation from depth toward the surface was observed. After the onset of most Hekla eruptions, the dominant seismic signal is volcanic tremor, which starts when the magma reaches the surface and continues with diminishing magnitude until the end of the eruption [*Soosalu et al.*, 2005].

[4] Various seismic and geodetic studies have addressed the existence and location of a magma chamber under Hekla.

Geodetic studies from optical levelling tilt [*Tryggvason*, 1994], EDM (electronic distance measurements) [*Kjartansson and Grönvold*, 1983], GPS measurements [e.g., *Sigmundsson et al.*, 1992] and borehole strain [*Linde et al.*, 1993], have inferred a magma chamber in the range of 5–11 km depth, with considerable associated uncertainty. On the other hand, *Soosalu and Einarsson* [2004] concluded that due to a lack of S wave attenuation under Hekla, a considerable molten volume cannot exist in the 4–14 km depth range. Individual interferometric synthetic aperture radar images (conventional InSAR) have been used to infer a broad preeruptive inflation centered on Hekla, about 40 km in diameter, with line-of-sight (LOS) shortening rates less than 10 mm/yr [*Sigmundsson et al.*, 2001]. These also show that a LOS lengthening signal, most pronounced over recent lava fields, is superimposed on the inflation signal and therefore masks uplift close to the summit. Previous geodetic studies in relation to the 26 February to 8 March 2000 eruption of Hekla indicate a deep seated magma source (≥10 km) and a shallow dike, connected by a narrow feeder channel [*Ágústsson et al.*, 2000; *Sturkell et al.*, 2005]. The aforementioned studies rely mostly on spatially sparse data sets, making it difficult to constrain the complex and extensive deformation field observed in the vicinity of the volcano. Only part of the Hekla area remains coherent in interferograms, necessitating a more thorough analysis. We use interferometric time series analysis of SAR data to study crustal deformation during 1993–2008. The time series includes the 2000 eruption and most of the intereruptive period between the 1991 and 2000 eruptions, as well as 8 years following the 2000 eruption.

2. SAR Data and Analysis

[5] Due to the small deformation rates spread over a large area and complex geometry of the deformation field around Hekla volcano, reduction of the impact of noise in the InSAR data on our inversions is essential. Multitemporal InSAR techniques reduce the effect of noise due to atmospheric distortions and orbital inaccuracies by filtering in time and space, as well as estimating errors introduced by inaccuracies in the model used for surface topography. Such methods also reduce the impact of decorrelation noise by selecting only the most coherent pixels for analysis. We analyzed the data with the STaMPS approach [*Hooper*, 2008], which uses the ROI-PAC software [*Rosen et al.*, 2004] to focus raw radar images, and the DORIS software [*Kampes and Usai*, 1999] to form the interferograms. STaMPS combines both the persistent scatterer (PS) and small baseline (SB) approaches. Spatial correlation of interferogram phase is used to find pixels with low-phase variance in all terrains. These pixels are then used to determine the evolution of crustal movements over time. With STaMPS, good results can be achieved in nonurban areas, and the combination of PS and SB approaches enables the extraction of signal from more pixels than either method alone. The detailed processing procedure is reported by *Hooper et al.* [2007] and *Hooper* [2008]. After forming interferograms using the DORIS software, candidate pixels are chosen based on their amplitude stability. The phase stability is estimated for each of the candidate pixels and coherent pixels are then selected based on both amplitude and phase stability. The effect of atmospheric phase delay in the reference SAR image is estimated as the signal present in every interferogram. Spatially correlated error in the digital elevation model (DEM) and errors due to incorrect mapping of the DEM are estimated from their correlation with the perpendicular component of the interferometric baseline. We did not subtract slave atmospheric signal and orbit errors from individual interferograms (Figures 2–4). We did however estimate a bilinear ramp from the mean rates to account for orbit errors and long-wavelength atmospheric signal. The ramp is an estimation of a signal that has a wavelength much greater than the whole image, therefore not significantly influencing the observed inflation signal. We used SAR data from the ERS-1 and ERS-2 satellites collected during 1993–2000, with a total of 27 acquisitions from descending track 52, and 17 acquisitions from ascending track 359. For the 2003–2008 period, we used 15 acquisitions from descending track 324 of the Envisat satellite. The LOS range change derived from the data, is shown in Figures 2–4. The time series from each track can be combined to reveal the mean LOS velocity for each of the three tracks, leading to a better estimate of crustal movements around Hekla.

[6] Maps of mean LOS velocities for the 1993–1999 and 2003–2008 periods for the three different tracks (Figure 5) all show a broad area of LOS shortening (inflation) approximately 20 km in radius, with LOS lengthening of up to 5–11 mm/yr close to the summit, forming a torus-like pattern. The LOS shortening around Hekla gradually increases from the edges of the study area toward the volcano to within ~6 km, where it starts to decrease until it becomes LOS lengthening at ~3 km from the summit (Figure 6). Both before the 2000 eruption (1993–1999) and after (2003–2008), the highest uplift rates (~6 km from the summit) are on the order of 2.5–5 mm/yr LOS. The images in Figures 2–5 are referenced to the southwest corner of the study area. This is the most stable area for the whole period prior to and after the M6.6 earthquakes in South Iceland in June 2000 [e.g., *Pedersen et al.*, 2001, 2003]. The deformation signal associated with these earthquakes is observed in the southwest corner of the last three interferograms in Figure 2 which span 21 July to 29 September 2000. A second center of LOS lengthening is apparent at Mt. Torfajökull near the eastern edge of the study area (Figure 5). This signal is observed in both the 1993–1999 and 2003–2008 LOS velocity fields. An aseismic volume of 4 km^3 at a center depth of 8 km, observed below the western part of the Torfajökull caldera, has previously been interpreted as a cooling magma body [*Soosalu and Einarsson*, 1997, 2004]. This interpretation is consistent with the subsidence observed at Torfajökull.

[7] To evaluate the temporal evolution of the deformation field, we examine the evolution of LOS range changes in ten small circular areas distributed evenly over the area of highest uplift rate (shown in Figure 5). We evaluate the mean of all the pixels within the area of each circle (50 m radius). We then calculate the average of those 10 points for each image in the descending displacement time series (Figures 2 and 4). The biases introduced due to different geometries are negligible as the horizontal contributions to the LOS on opposite sides of Hekla approximately cancel each other out. In track 52 a constant uplift rate of

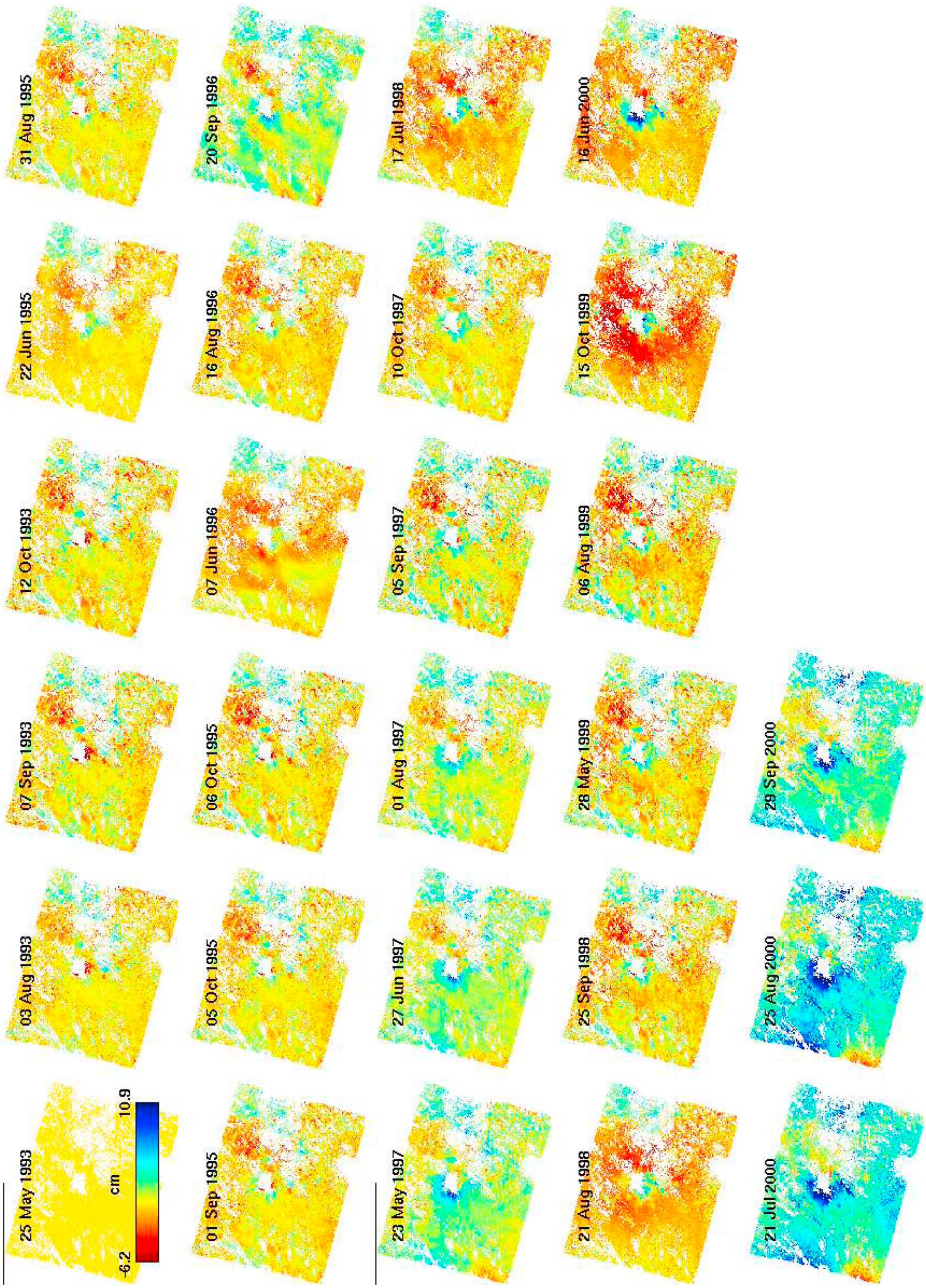

Figure 2. The 1993–2000 time series of LOS unwrapped phase change relative to the first image (in cm). Phase due to master atmospheric delay and DEM errors in the master interferogram has been estimated and removed. The interferograms are based on 27 acquisitions by the ERS-1 and ERS-2 satellites from track 52. A minus on the scale bar represents shortening LOS range.

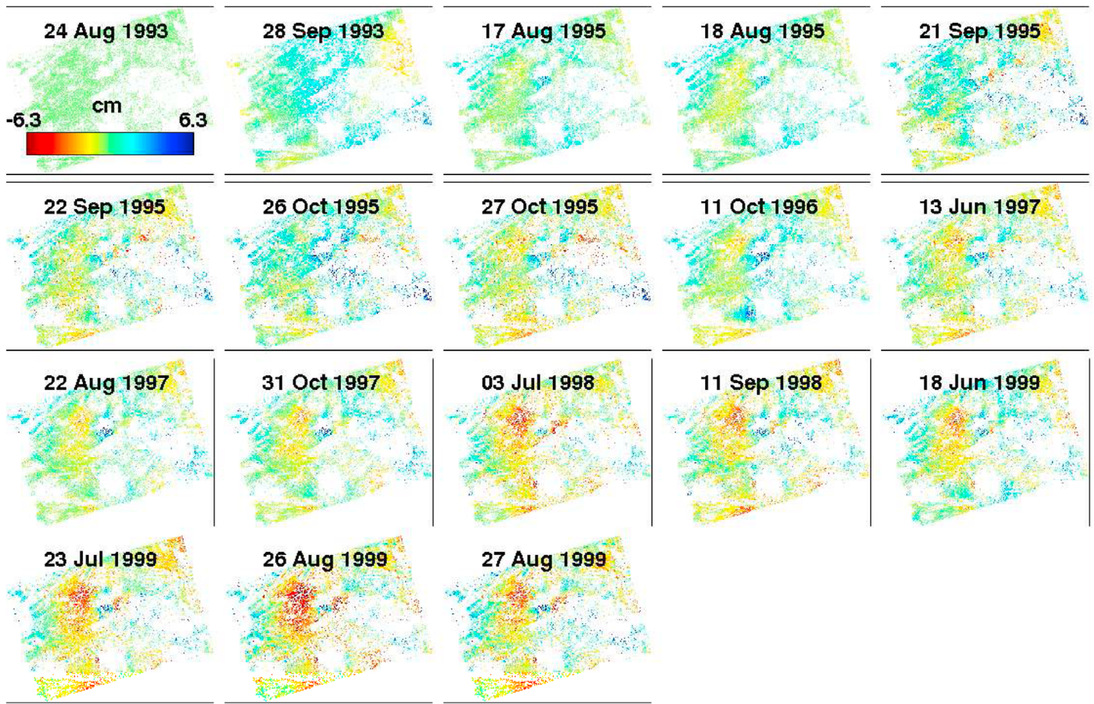

Figure 3. The 1993–2000 time series of LOS unwrapped phase change relative to the first image (in cm). Phase due to master atmospheric delay and DEM errors in the master has been estimated and removed. The interferograms are based on 17 acquisitions from the ERS-1 and ERS-2 satellites from track 359. A minus on the scale bar represents shortening of LOS range.

(3.3 ± 0.7) mm/yr is observed during 1993–1999 and after the 2000 eruption, an offset of −17 mm is observed (Figure 7). In track 324, covering the 2003–2008 period, we infer rates of (3.4 ± 2.0) mm/yr, similar to the earlier period but with larger uncertainty. Despite the lack of data for the 2000–2003 interval, the data series suggest that the rates in the interval 1993–2008 are approximately constant, except during the 2000 eruption.

[8] The coeruptive displacements, observed in the 245 day interval between the 15 October 1999 and 16 June 2000 acquisitions (Figure 8), show about 17 mm subsidence in the area of peak intereruptive inflation. Superimposed on the deflation is a local signal centered on the volcano, elongated parallel to the eruptive fissure. The symmetry around the eruptive fissure, and the limited spatial scale of that signal, suggest that a shallow dike fed the eruption (Figure 8).

3. Model

[9] The deformation field around Hekla in the periods before and after the 2000 eruption is complex. The torus-like inflation has an irregular structure, especially close to the summit. The extent of recent pre-2000 lava fields correlates partly with areas of subsidence observed in the mean LOS velocity field of track 52 during 1993–1999 (Figure 9). This is likely partly due to thermal contraction of the lava as it cools. However, cooling of recent lava can only explain part of the subsidence, as the LOS lengthening, around the summit area reaches beyond the outlines of the lava flows (Figure 9). The broad nature of the subsidence may be due to the load of the volcano and its recent lava fields [*Grapenthin et al.*, 2010], although the possibility of a shallow deflating magma source cannot be discarded.

[10] The shape of the broad inflationary deformation field is approximately radially symmetric. We therefore modeled the signal with a spherical magma chamber in an elastic half-space. Its approximate solution is given by that for a point pressure source [*Mogi*, 1958]. We also explored modeling the signal with a horizontal penny shaped crack [*Fialko et al.*, 2001], but the surface deformation associated with the best fit deviated considerably in shape from the data. We assumed a Poisson's ratio of 0.25 and a Young's modulus of 30 GPa [*Grapenthin et al.*, 2006; *Pinel et al.*, 2007], and used the LOS velocities to estimate the depth and rate of volume change of the pressure source. A Markov chain Monte Carlo sampling algorithm was applied to find the posterior probability distribution of the model parameters [*Mosegaard and Tarantola*, 1995]. The method was applied to three data sets: ERS track 52 data for the 1993–1999 period, ERS track 52 data for the 15 October 1999 to 16 June 2000 period spanning the 2000 eruption of Hekla, and Envisat track 324 data for the 2003–2008 period. As ERS and Envisat cover different time intervals modeling them individually enables us to compare the results from the two intervals. Fewer coherent pixels were found for track 359 due to the unfavorable distribution of acquisitions with respect to time and satellite position. This can influence the quality of the phase unwrapping, eventually biasing modeling results.

[11] We took two different approaches to account for the superimposed contributions of different deformation sources: First, we masked out the central subsidence and the

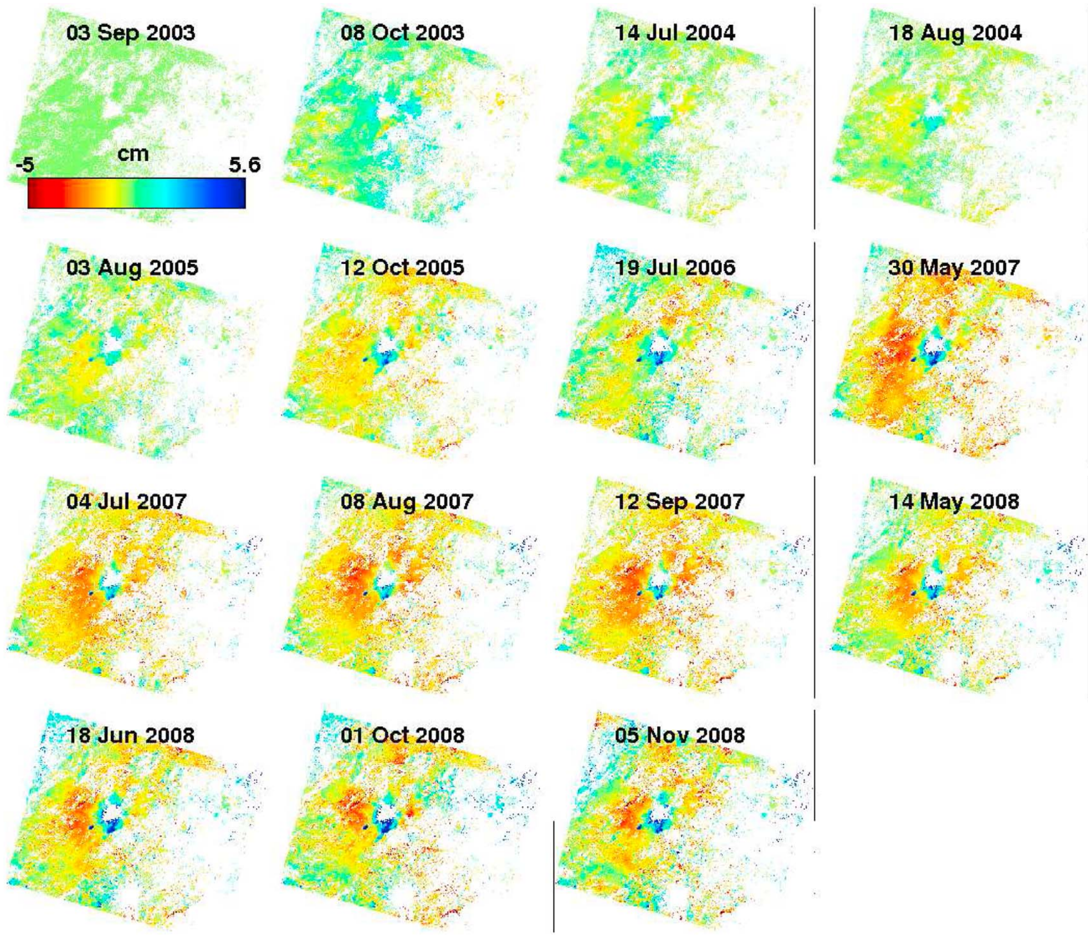

Figure 4. The 2003–2008 time series LOS unwrapped phase change relative to the first image (in cm). Phase due to master atmospheric delay and DEM errors has been estimated and removed. The interferograms are based on 15 acquisitions by the Envisat satellite from track 324. A minus on the scale bar represents shortening of LOS range.

coeruptive fissure on the assumption that the effects of these features are negligible in the far field. Second, we modeled the deformation due to lava loading and dike formation during the eruption.

[12] When inverting for the model parameters of the preeruptive signal, a circular area with 9 km radius centered on the summit as well as an elliptical area over Torfajökull were masked out to prevent the subsidence signals around Hekla and Torfajökull from influencing the model. Marginal posterior probability distributions for the depth and volume change of a spherical source model are shown in Figure 10. The resulting model parameters for depth and volume change are shown in Table 1. For the coeruptive deflation modeling a circular area with 6 km radius around Hekla's summit was masked out to eliminate deformation associated with the eruptive fissure. The observed LOS velocity, model and residual are shown in Figure 11. The inversions of all the data sets show the same result, with source depths of 14–20 km. The rates of volume increase for the 1993–1999 and 2003–2008 periods are also comparable, with rates 0.003–0.015 km^3/yr. The deflation observed in the coeruptive interval suggests a volume decrease of 0.04–0.08 km^3, which is similar to the accumulated volume of the 1993–1999 and 2003–2008 time periods. In both cases, the source is located at (19.6434°W, 63.9880°N), just below eastern part of Hekla's summit.

[13] We evaluated two different mechanisms for the central subsidence close to Hekla. First, we explored if it could be attributed to a shallow magma source. We inverted for an additional shallow, spherical (see above), deflating source to account for the outer part of the central subsidence but the results do not compare well with the observed data. In addition, there is no pressure decrease at shallow depth observed in the data for the coeruptive period, as would be expected if magma drained from there during the eruption. Second, we investigated viscoelastic relaxation due to lava loading as a source for the central subsidence as suggested by *Grapenthin et al.* [2010].

[14] In order to estimate the load signal we use the approach suggested by *Grapenthin et al.* [2010]. First we calculate uplift due to the modeled magmatic source (that was estimated only from the part of the signal that is not significantly influenced by the loading), then we estimate the difference in displacement between the modeled source

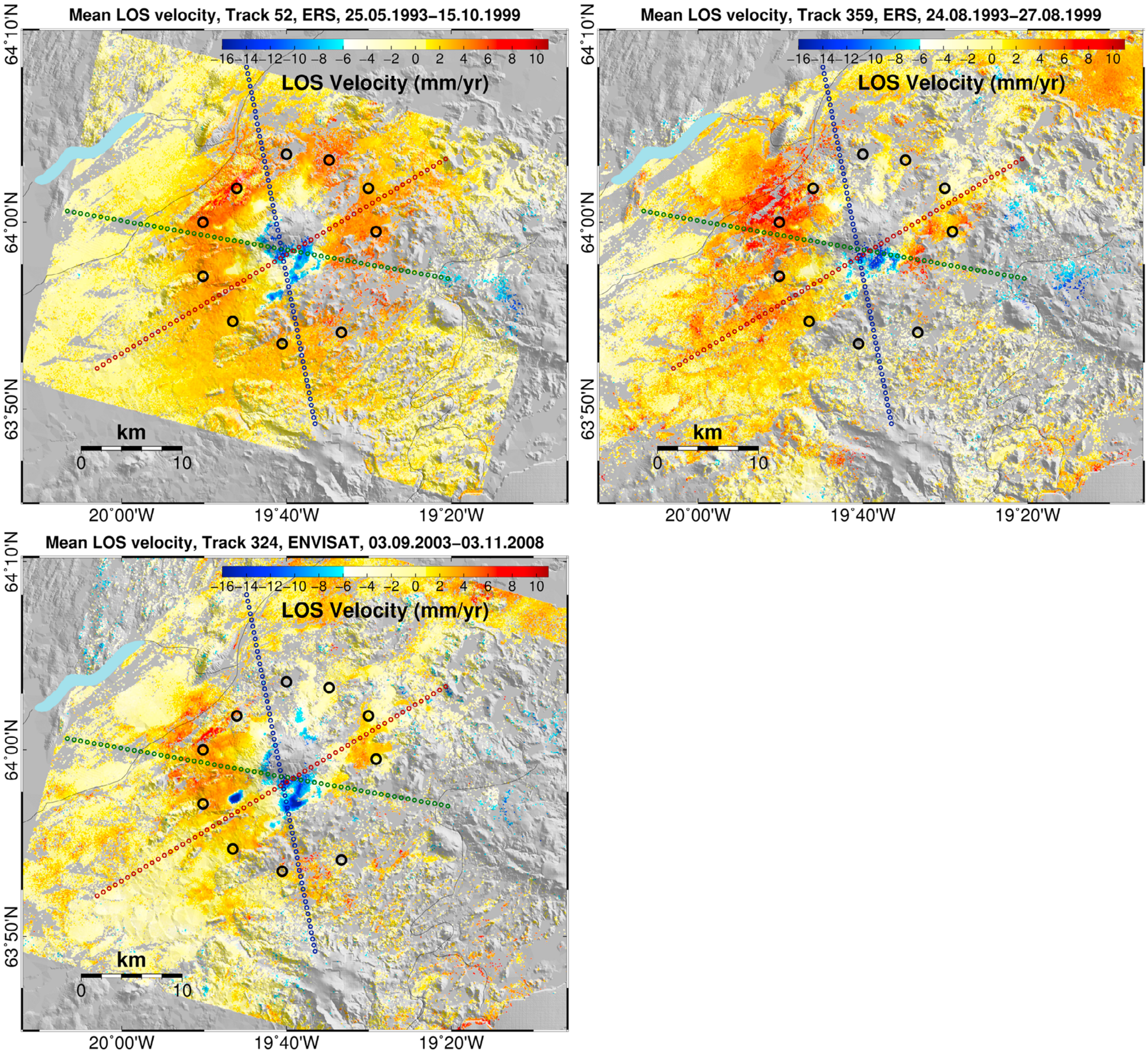

Figure 5. Mean LOS velocities before and after the 2000 eruption. Deformation associated with the 2000 eruption is not included. (a) Track 52, descending orbit. (b) Track 359, ascending orbit. (c) Track 324, descending orbit covering the time interval after the 2000 eruption. The lines of colored dots correspond to the profiles shown in Figure 6. The black circles, aligned around the summit approximately where the highest LOS shortening is observed, are locations used in Figure 7. The deformation around Hekla is torus-like, with uplift rates peaking around 6 km from the summit and then decreasing toward the summit and becoming subsidence. A second center of subsidence is observed east of Hekla, at Torfajökull. A minus sign on the scale bar represents lengthening of LOS range.

and the observations. This difference together with the radius of the central subsidence can be used to estimate the crustal parameters necessary to infer current displacement rates due to recently emplaced lava flows.

[15] We first calculated a difference of about 13.5 mm/yr in LOS velocity between the LOS lengthening outside the lava flows and our best fitting Mogi source from the model described above (17 km depth and volume rate of 0.01 km^3/yr; Figure 6 dashed line). This serves as a conservative estimate of subsidence rates induced by surface loading around Hekla. Next, we performed a grid search over the elastic thickness and effective relaxation time to find values that fit the observed radius of the central LOS lengthening and the velocity of 13.5 mm/yr, respectively. In this process we calculated the crustal response to the individual lava loads defined by an average thickness, their spatial extent and time of emplacement. The average thickness of individual lava flows (varying from 3.8–34.6 m between different flows) is estimated by *Grapenthin et al.* [2010] using volume estimates and lava areas of *Höskuldsson et al.* [2007]. The

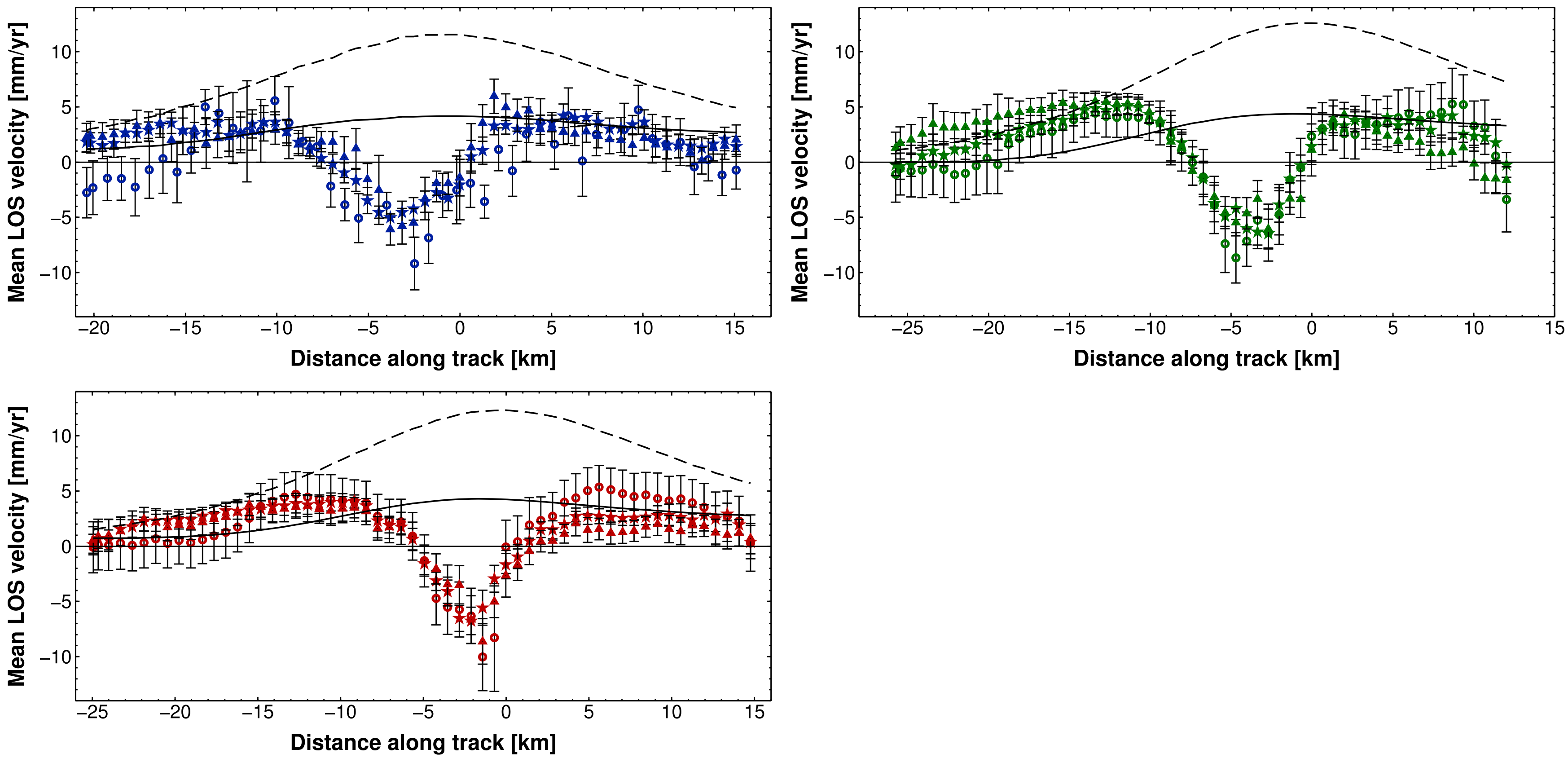

Figure 6. Velocity profiles across the deformation field at Hekla. The colors indicate the location of the profiles shown in Figure 5. The circles are from track 52, triangles from track 359, and asterisk from track 324. The profiles indicate the width of the inflation, which is at least 30 km, and the superimposed subsidence at the summit area extending to 6 km distance from the summit. The black hatched line is the LOS part of the estimated spherical source at 17 km depth with 0.01 km^3/yr volume increase. The black solid line is the LOS change due to a spherical source with estimated LOS displacements due to loading [*Grapenthin et al.*, 2010] subtracted. The Mogi source has 16 km depth and 0.02 km^3/yr volume rate.

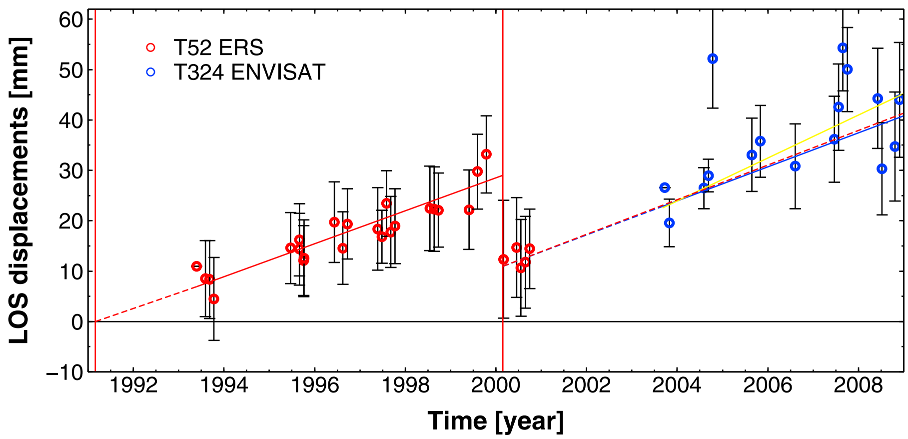

Figure 7. Average LOS time series of areas selected from the descending (ERS track 52 and Envisat track 324) InSAR time series spanning 1993–2008. The location of 10 circular areas used to construct this time series are shown in Figure 5 (black circles distributed along the area of highest LOS shortening). We calculate the average value within each of these 10 circles and then the average of these values for each track. The red vertical lines show the beginning of the 17 January 1991 and 26 February 2000 eruptions. Before the 2000 eruption, a steady rate of (3.3 ± 0.7) mm/yr LOS rate is inferred (from the track 52 data, red line). A similar rate is inferred after the eruption, (3.4 ± 2.0) mm/yr (blue line). The dotted red line is a continuation of the fit for the track 52 data (1993–1999), an offset of –17 mm LOS occurred as a result of Hekla's 2000 eruption.

superposition of these individual responses provides a model for the load-induced deformation signal. Although the relaxation time depends on the load wavelength, the similar spatial extent of the lava flows from 1947–1991 allows us to infer a single effective relaxation time of t_r = 100 yr and a best fitting elastic plate thickness of H = 3.5 km [*Grapenthin et al.*, 2010]. Using these values we removed the load contribution (converted to LOS velocity) from the observed displacement field and inverted the result for a spherical source again. This procedure gives an estimate for an inflation source at a depth of 16 km with a volume rate of 0.02 km^3/yr located at (−19.703°W 63.988°N) below the western part of Hekla's summit. The fit to the data is improved considerably using this method (Figure 6, solid line). We have taken an approach of iterative modeling of the magma source and loading because of its simplicity. A joint inversion would be more difficult and require a different approach than we have taken. Our result should not differ (within uncertainty) from an alternative joint inversion as the first estimation of a magma source is made using part of the data that is not significantly influenced by the loading. However, a joint inversion would probably reduce the margin of error.

[16] Deformation due to the feeder dike of the 2000 eruption has also been considered. Interferograms spanning the 2000 eruption exhibit a deformation pattern around Hekla indicating movement away from the satellite on the NW side and toward the satellite on the SE side (Figure 8), which we modeled in terms of dike emplacement. We used only the interferogram from October 1999 to September 2000, which has the maximum coherence and thus minimizes the chance of phase-unwrapping errors. In the forward model, we used the elastic Green's functions for a rectangular dislocation [*Okada*, 1985] and accounted for topography using the perturbation approach of *Williams and Wadge* [2000]. To account for orbit errors and long-wavelength atmospheric signal, we estimated a bilinear (ramp) using least squares for an area of the interferogram that excludes deformation due to the eruption and the earthquakes of June 2000. We subtracted the ramp and estimated the variance-covariance of the remaining atmospheric signal from the same area, by calculating the experimental variogram and fitting a spherical covariance model. As in our previous modeling, we set the problem up in a Bayesian fashion and applied Markov chain Monte Carlo sampling to build the posterior distribution of our model parameters. We find that opening alone cannot explain the deformation signal, even if we allow the amount of opening to vary in both strike and dip directions. This is because the horizontal displacement caused by opening on the NW side is approximately canceled by the vertical displacement when the two are combined in the LOS direction. When we allow slip on the dike walls, the data are somewhat better fit. The depth to the bottom is not well constrained, and trades off with dip (lower dip implies shallower depth). A uniform opening and strike-slip model results in a total intruded volume of 0.005–0.006 km^3. The position and strike match well with the eruptive fissure (Figure 8). The dike model reaches a depth of up to 5.8 km below sea level, with dip of 70–73°SE, opening of 18–23 cm and left-lateral slip of 23–31 cm at 95% confidence.

4. Results and Discussion

[17] Previous geodetic studies at Hekla have resulted in a wide range of depth estimates for a magma source under the volcano. Optical levelling tilt measurements led *Tryggvason* [1994] to suggest a magma source centered 4–6 km northwest of the summit but at 5–6 km depth. EDM measurements published by *Kjartansson and Grönvold* [1983]

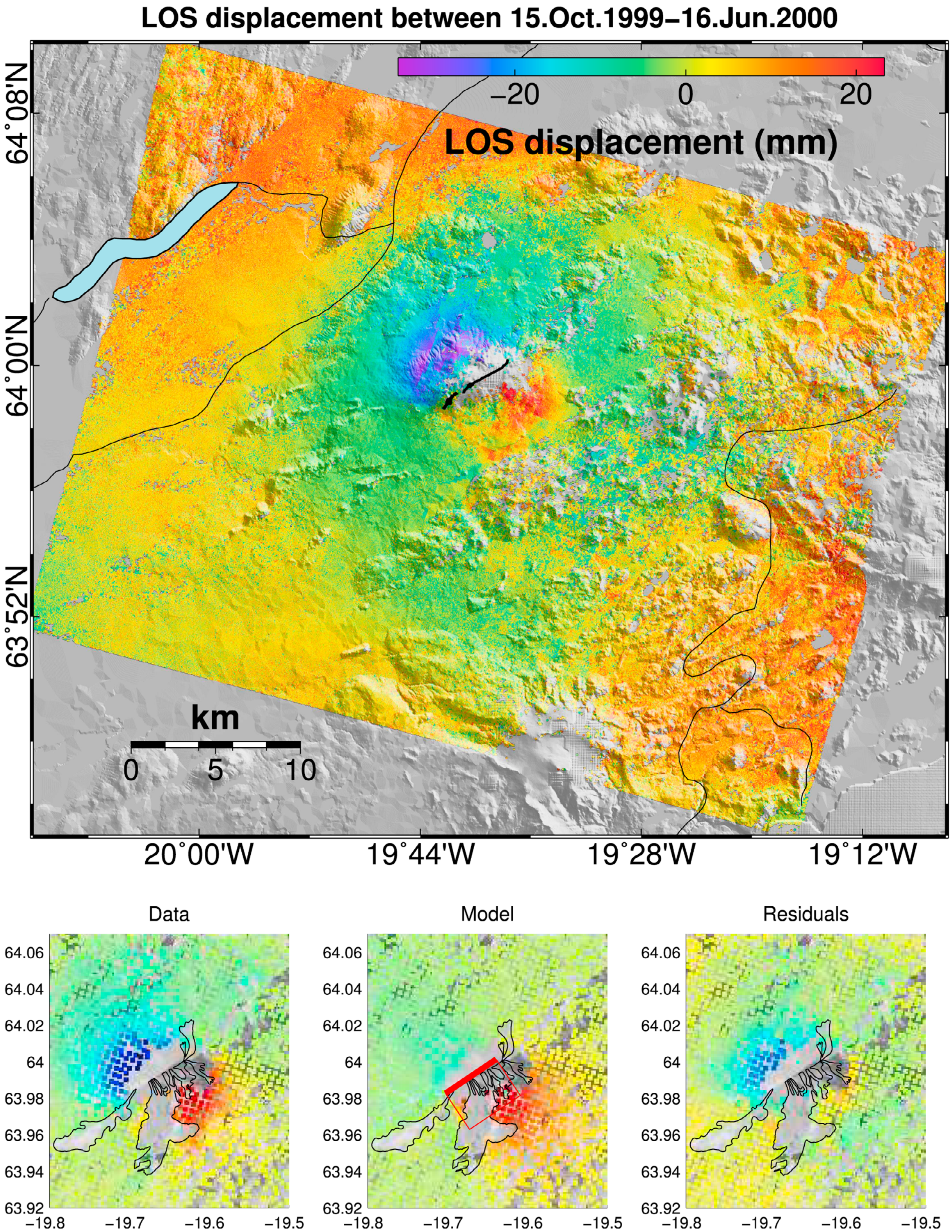
LOS displacement between 15.Oct.1999–16.Jun.2000
−20
0
20
LOS displacement (mm)
64°08'N
64°00'N
63°52'N
km
0
5
10
20°00'W
19°44'W
19°28'W
19°12'W
Data
Model
Residuals
64.06
64.04
64.02
64
63.98
63.96
63.94
63.92
−19.8
−19.7
−19.6
−19.5

Figure 8

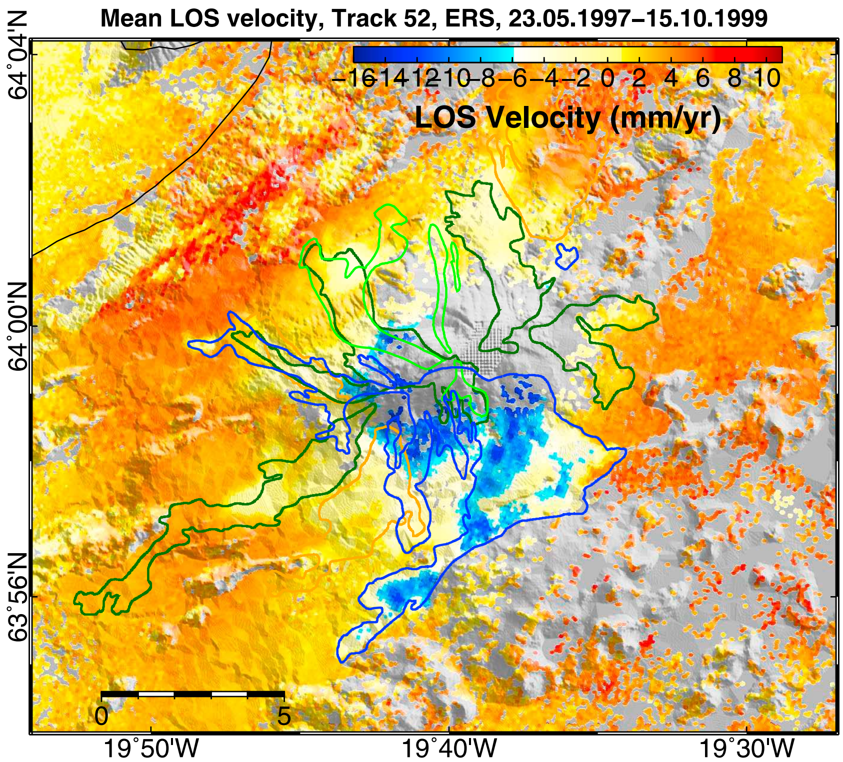

Figure 9. Mean LOS velocity proximal to Hekla from ERS track 52 with outlines of recent lava flows. Dark green outlines the 1980 lava field, bright green outlines the 1981 lava field, and blue outlines the 1991 lava field. Some of the LOS lengthening correlates with the recent lava flows.

suggested a 8 km deep source below the summit. Early GPS measurements presented by *Sigmundsson et al.* [1992] were indicative of a source in the 2–15 km depth range, poorly constrained due to a lack of GPS stations close to Hekla. A study of coeruptive borehole strain data by *Linde et al.* [1993] initially suggested a 6.5 km deep source, but that depth was revised to about 10 km in a later study [*Sturkell et al.*, 2005]. With conventional InSAR studies [*Sigmundsson et al.*, 2001], the complexity of the deformation field around Hekla was noted, but detailed modeling of the data was not conducted. Previous results appear to be influenced by the complex nature of the deformation field around Hekla and insufficient spatial sampling by the deformation data.

[18] For the 1993–1999 and 2003–2008 intervals, a simple spherical pressure source model, at a depth of (17 ± 3) km fits the long-wavelength deformation observed by InSAR fairly well. The observed deflation from the coeruptive signal shows the same source depth of (16 ± 2) km. This is deeper than most previous geodetic studies have suggested, but it is in accordance with seismic studies, which argue against a sizable molten body in the depth range of 4–14 km. Removing the deformation due to the best fit spherical magma model from the deformation data results in residual LOS velocities that indicate superimposed LOS subsidence at a rate of 14–20 mm/yr, centered on the summit area.

[19] Although the LOS lengthening centered on Hekla partly masks the inflation signal, the spatial extent of the LOS lengthening is limited and has only a small effect on the inferred source depth. A model that estimates the viscoelastic relaxation due to the load of the recent lava flows from the data, as suggested by *Grapenthin et al.* [2010], explains a substantial part of the LOS lengthening observed outside the lava fields (Figure 6). Subtracting the estimated deformation due to this load model from the data results in a shifted pressure source at a similar depth, but with twice the volume rate compared to inversion without taking load effects into consideration.

[20] Although we do not model the LOS lengthening observed within the recent lava fields, the strong correlation between the LOS lengthening and outlines of the lavas

Figure 8. (top) LOS coeruptive displacements between 15 October 1999 and 16 June 2000 from descending track 52. A broad area around the volcano is characterized by displacement away from satellite, about 15–20 mm relative to the surroundings. The local deformation signal that straddles the summit is due to the formation of the 2000 eruptive fissure (black line on the summit) and is superimposed on widespread coeruptive LOS deflation. (bottom left) LOS coeruptive displacements between October 1999 and September 2000, showing the coeruptive signal surrounding the eruptive fissure. (bottom middle) The best fit uniform opening and strike-slip model shown in red. The total intruded volume is estimated at 0.005–0.006 km^3. The dike reaches to a depth of up to 5.8 km below sea level with a dip of 70–73°SE and opening of 18–23 cm, with left-lateral slip of 23–31 cm. (bottom right) Residuals of the displacements and the dike model.

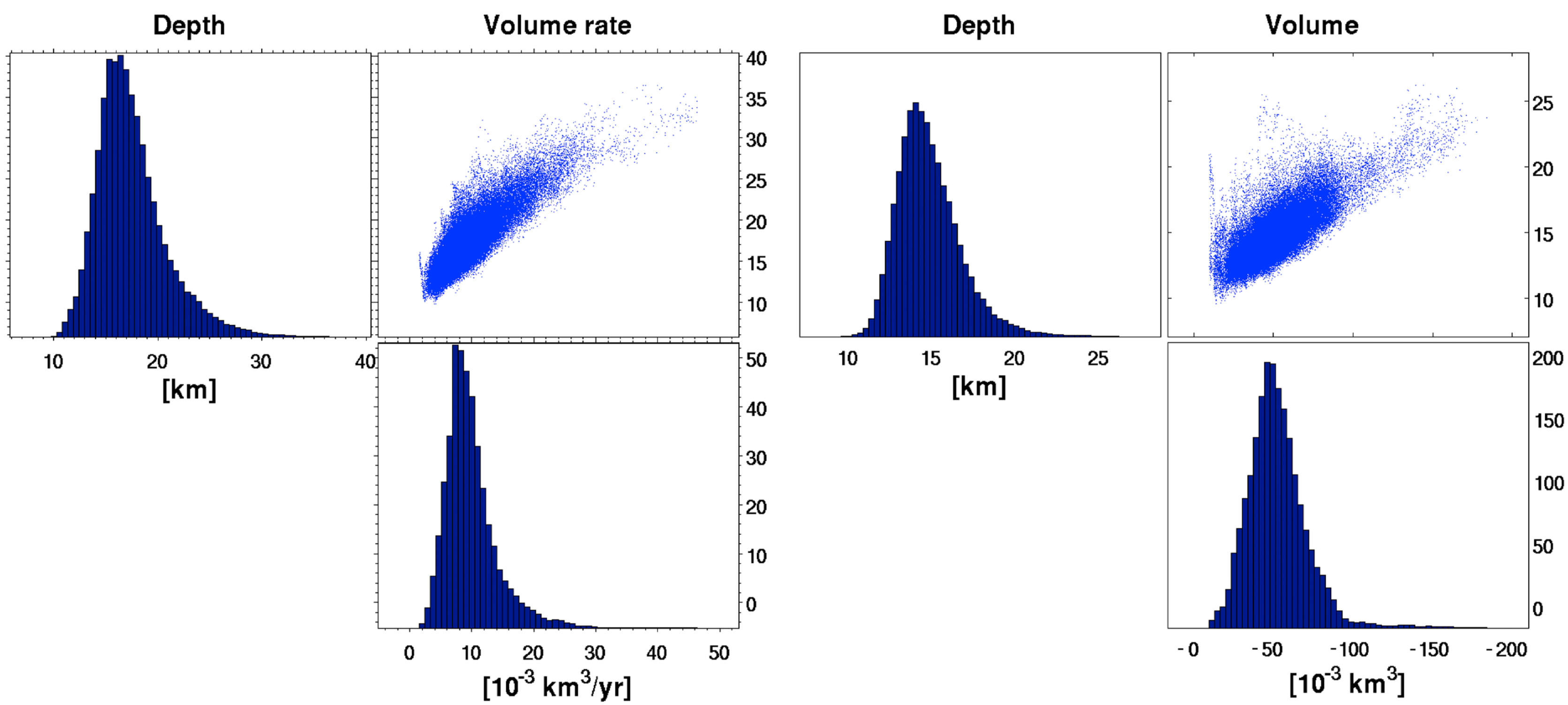

Figure 10. Marginal posterior probability distributions for the center depth and volume change of a Mogi source. The histograms show the distributions for individual parameters, and the scatterplots show distributions for each pair of parameters. (left) The distributions of depth and volume rate for 1993–1999 derived from track 52 (see Figure 5). (right) The distributions for depth and net volume contraction of the magma chamber based on the coeruptive signal (see Figure 8).

Table 1. Optimum Model Parameters Found From ERS, Track 52, 1993–1999, and Coeruptive Displacement As Well As 2003–2008 Period From Track 324 of Envisat[a]

Optimum Model Parameters			
Track	Period	Depth (km)	Volume Rate (km^3/yr)
52	1997–1999[b]	17 ± 3	0.010 ± 0.005
	1999–2000[c]	16 ± 2	0.06 ± 0.01[d]
324	2003–2008[e]	17 ± 2	0.005 ± 0.002

[a]The analyzed InSAR data set is consistent with a magma chamber beneath Hekla, modeled as spherical source in elastic half-space, with a center depth of 17 ± 3 km.
[b]From 23 May 1997 to 15 October 1999.
[c]From 15 October 1999 to 16 June 2000, coeruptive displacement.
[d]Volume in km^3.
[e]From 3 September 2003 to 3 November 2008.

suggests a process operating within the lava fields themselves. The strongest signal is observed on the most recent lavas suggesting thermal contraction of these cooling lavas. For the coeruptive signal surrounding the eruptive fissure (Figure 8), a uniform opening and strike-slip model results in a total dike intruded volume of 0.005–0.006 km^3. The dike reaches a depth of up to 5.8 km below sea level, with dip of 70–73°SE, opening of 18–23 cm and left-lateral slip of 23–31 cm. The dike does not extend down to the depth of the inferred magma source. This is consistent with the model of *Sturkell et al.* [2005], who suggested that the 2000 feeder dike and the deep magma source were connected by a narrow feeder channel that does not cause significant deformation.

[21] Between eruptions, our results indicate that magma flow into the inferred deep chamber is at a constant rate, as deformation rates are approximately linear (Figure 7). Until now, the best indication of inflation around Hekla has been from optical levelling at the Næfurholt (NAEF) tilt station (Figure 12). The east component of tilt at that site is sensitive to the inflation and deflation of a magma chamber beneath Hekla. Although the NAEF tilt station has proven to be a good long-term indicator of pressure changes within Hekla's magma chamber, it measures ground tilt at only one location. The inflation/deflation pattern at the NAEF tilt station is, however, similar to the pattern inferred from InSAR (Figure 7). The InSAR time series is based on few thousand pixels distributed over the area of highest LOS shortening around the volcano, which makes it less sensitive to local disturbances that may characterize data from a single tilt station.

[22] It is becoming evident from geodetic studies that at some volcanic systems in Iceland deep magma storage (≥10 km) occurs beneath a shallow magma chamber (≤5 km). There are other cases of such dual magma systems, such as at Soufrière Hills volcano on Montserrat where *Elsworth et al.* [2008] suggest dual magma chambers at 6 and 12 km. The deeper sources are either near, or below, the brittle-ductile transition in the crust. Hekla, however, appears different from these dual magma chamber systems as we only

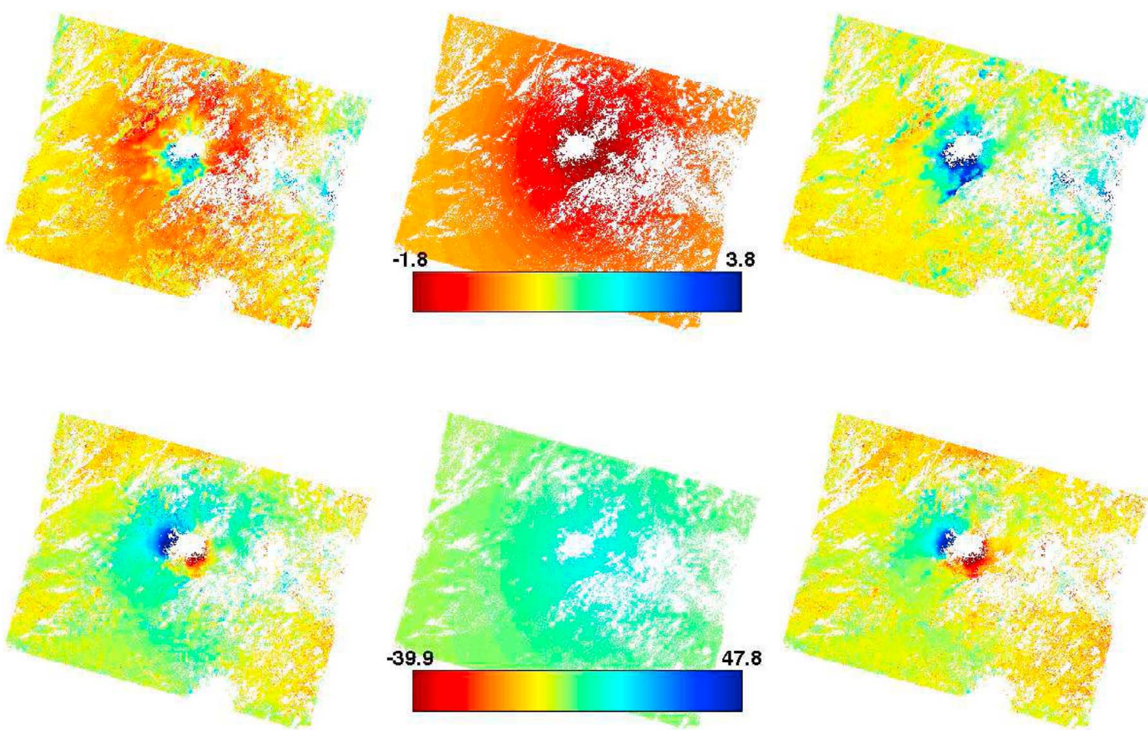

Figure 11. (left) LOS velocities (mm/yr) as shown in Figures 5 (top left) and 8 (top). (middle) The corresponding optimal Mogi model. (right) Residual plot. (top) Images showing the 1993–1999 time series and (bottom) images showing the coeruptive signal (15 October 1999 to 16 June 2000) from track 52 in both cases. The Mogi model used is the optimal for each case. For the 1993–1999 period, the modeled source is at a depth of 17 km and has a volume rate of 0.01 km^3/yr, and for the coeruptive period it is at a depth of 16 km with a volume decrease of 0.06 km^3.

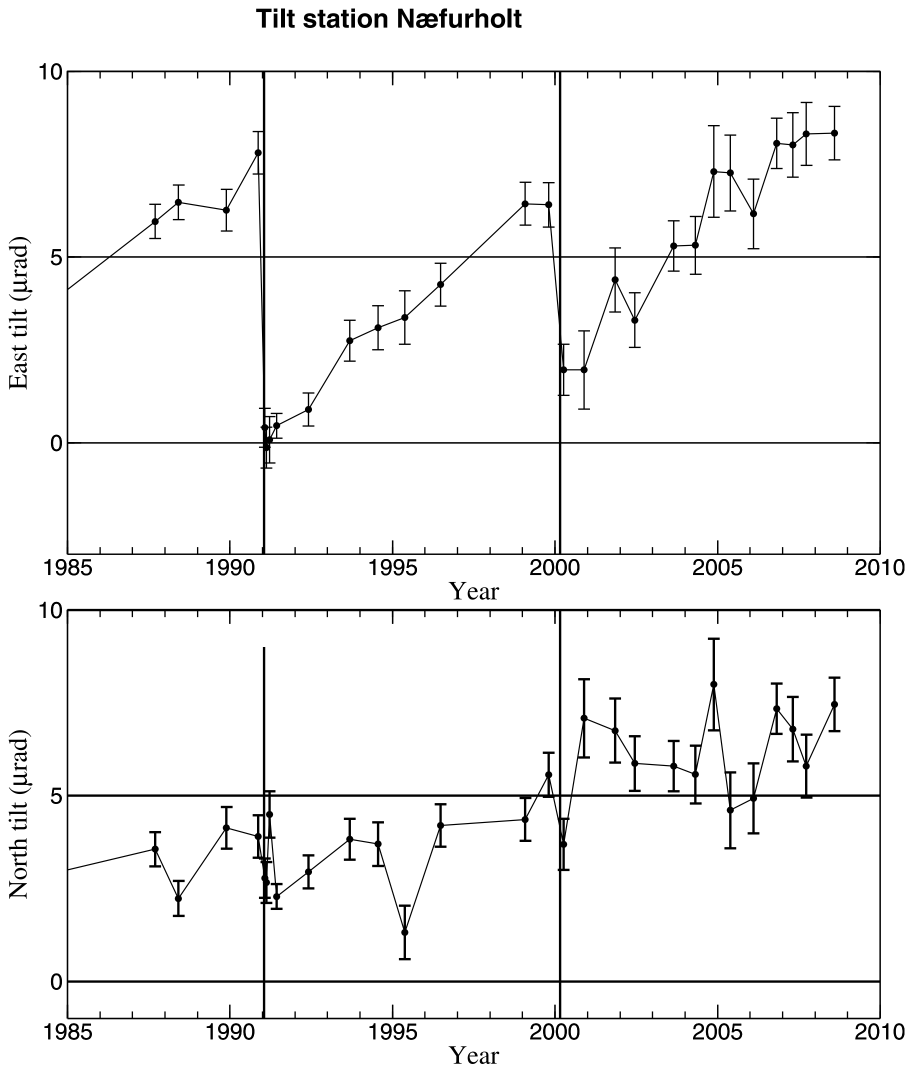

Figure 12. Time series of tilt from the NAEF station (see Figure 1 for location). Vertical lines indicate eruptions. The north component is tilting slowly to the north, not showing any changes during the two eruptions. The east component shows a "sawtooth" pattern. A continuous upward tilt toward Hekla of ~0.7 μrad/yr occurs between eruptions, and the signal is reversed during eruptions. A southward tilt of about 5–8 μrad during the 1991 and 2000 eruptions was observed.

find evidence for a single deep source. Further modeling of such deep sources should account for variable crustal properties. Importantly, for a deep magma source, a more detailed model should account for viscoelastic yielding and possible crustal layering.

5. Conclusions

[23] Multitemporal InSAR analyses give promising results for monitoring small deformation rates over large areas. The preeruptive 1993–2000 period at Hekla volcano, is characterized by inflation at a constant rate. Superimposed on this inflation is a central LOS lengthening with a maximum rate of 20 mm/yr. The subsidence is inferred to be a result of thermal contraction of recent lava flows, as well as viscoelastic yielding due to loading by the volcano and its lavas. The 2003–2008 interval shows the same characteristics as the 1993–2000 interval. The broad inflation signal that characterizes Hekla in the 1993–1999 and 2003–2008 periods has a radius of approximately 20 km with an inferred source depth in the range of 14–20 km. Interferograms spanning the time of the 2000 eruption indicate deformation related to the opening of a shallow dike with a volume of 0.005–0.006 km^3. The dike is superimposed on coeruptive deflation of approximately 20 km radius with an estimated source depth of 14–18 km. Our modeling can explain both, the broad area of inflation at Hekla in the 1993–1999 and 2003–2008 intervals, and the observed deflation during the 2000 eruption. The broad deformation is consistent with a pressure change in a deep seated magma source centered in the 14–20 km depth range under the volcano.

[24] **Acknowledgments.** The University of Iceland Research Fund, the Icelandic Research Fund through the Icelandic Center for Research (RANNÍS), and EU project VOLUME funded the work presented here. ESA provided the SAR data. R.G. was supported by NSF award

EAR-0409950 and the Alaska Volcano Observatory. Comments from Páll Einarsson and Thóra Árnadóttir helped to improve this paper.

References

Ágústsson, K., R. Stefánsson, A. T. Linde, P. Einarsson, S. I. Sacks, G. B. Gudmundsson, and B. Thorbjarnardóttir (2000), Successful prediction and warning of the 2000 eruption of Hekla based on seismicity and strain changes, *Eos Trans. AGU*, *81*(53), Fall Meet. Suppl., Abstract V11B-30.

de Zeeuw-van Dalfsen, E., R. Pedersen, F. Sigmundsson, and C. Pagli (2004), Satellite radar interferometry 1993–1999 suggests deep accumulation of magma near the crust-mantle boundary at the Krafla volcanic system, Iceland, *Geophys. Res. Lett.*, *31*, L13611, doi:10.1029/2004GL020059.

Einarsson, P. (1991), Earthquakes and present-day tectonism in Iceland, *Tectonophysics*, *189*, 261–279.

Einarsson, P., and K. Sæmundsson (1987), Earthquake epicenters 1982-1985 and volcanic systems in Iceland, map accompanying *Í hlutarins edli*, edited by T. I. Sigfússon, Menningarsjódur, Reykjavík.

Elsworth, D., G. Mattioli, J. Taron, B. Voight, and R. Herd (2008), Implications of magma transfer between multiple reservoirs on eruption cycling, *Science*, *322*(5899), 246–248, doi:10.1126/science.1161297.

Fialko, Y., Y. Khazan, and M. Simons (2001), Horizontal circular crack in an elastic half-space, with applications to volcano geodesy, *Geophys. J. Int.*, *146*, 181–190.

Grapenthin, R., F. Sigmundsson, H. Geirsson, T. Árnadóttir, and V. Pinel (2006), Icelandic rhythmics: Annual modulation of land elevation and plate spreading by snow load, *Geophys. Res. Lett.*, *33*, L24305, doi:10.1029/2006GL028081.

Grapenthin, R., B. Ófeigsson, F. Sigmundsson, and E. Sturkell (2010), Pressure sources versus surface loads: Analyzing volcano deformation signal composition with an application to Hekla volcano, Iceland, *Geophys. Res. Lett.*, *37*, L20310, doi:10.1029/2010GL044590.

Hooper, A. (2008), A multi-temporal InSAR method incorporating both persistent scatterer and small baseline approaches, *Geophys. Res. Lett.*, *35*, L16302, doi:10.1029/2008GL034654.

Hooper, A., P. Segall, and H. Zebker (2007), Persistent scatterer interferometric synthetic aperture radar for crustal deformation analysis, with application to Volcón Alcedo, Galápagos, *J. Geophys. Res.*, *112*, B07407, doi:10.1029/2006JB004763.

Hooper, A., B. G. Ofeigsson, H. Geirsson, F. Sigmundsson, P. Einarsson, and E. Sturkell (2008), Magma capturing in lower ductile crust: Reawakening of northern Iceland's divergent plate boundary, *Eos Trans. AGU*, *83*(59), Fall Meet. Suppl., Abstract V51D-2075.

Höskuldsson, Á., N. Óskarsson, R. Pedersen, K. Grönvold, K. Vogfjörd, and R. Ólafsdóttir (2007), The millennium eruption of Hekla in February 2000, *Bull. Volcanol.*, *70*, 169–182, doi:10.1007/s00445-007-0128-3.

Kampes, B., and S. Usai (1999), Doris: The Delft object-oriented radar interferometric software, paper presented at 2nd Operationalization of Remote Sensing Symposium, ITC, Enschede, Netherlands.

Kjartansson, E., and K. Grönvold (1983), Location of a magma reservoir beneath the Hekla volcano, Iceland, *Nature*, *301*, 139–141.

Linde, A. T., K. Agustsson, I. S. Sacks, and R. Stefansson (1993), Mechanism of the 1991 eruption of Hekla from continuous borehole strain monitoring, *Nature*, *365*, 737–740.

Mogi, K. (1958), Relation between the eruptions of various volcanoes and deformations of the ground surfaces around them, *Bull. Earthquake Res. Inst. Univ. Tokyo*, *36*, 99–134.

Mosegaard, K., and A. Tarantola (1995), Monte Carlo sampling of solutions to inverse problems, *J. Geophys. Res.*, *100*, 12,431–12,447.

Okada, Y. (1985), Surface deformation due to shear and tensile faults in a half-space, *Bull. Seismol. Soc. Am.*, *75*, 1135–1154.

Pagli, C., F. Sigmundsson, R. Pedersen, P. Einarsson, T. Árnadóttir, and K. L. Feigl (2007), Crustal deformation associated with the 1996 Gjálp subglacial eruption, Iceland: Insar studies in affected areas adjacent to the Vatnajökull ice cap, *Earth Planet. Sci. Lett.*, *259*(1-2), 24–33, doi:10.1016/j.epsl.2007.04.019.

Pedersen, R., F. Sigmundsson, K. Feigl, and T. Árnadóttir (2001), Coseismic interferograms of two MS = 6.6 earthquakes in the South Iceland Seismic Zone, June 2000, *Geophys. Res. Lett.*, *28*(17), 3341–3344.

Pedersen, R., S. Jónsson, T. Árnadóttir, F. Sigmundsson, and K. L. Feigl (2003), Fault slip distribution of two June 2000 Mw6.5 earthquakes in south Iceland estimated from joint inversion of InSAR and GPS measurements, *Earth Planet. Sci. Lett.*, *213*(3-4), 487–502, doi:10.1016/S0012-821X(03)00302-9.

Pinel, V., F. Sigmundsson, E. Sturkell, H. Geirsson, P. Einarsson, M. T. Gudmundsson, and T. Högnadóttir (2007), Discriminating volcano deformation due to magma move ments and variable surface loads: Application to Katla subglacial volcano, Iceland, *Geophys. J. Int.*, *169*, 325–338.

Rosen, P. A., S. Henley, G. Peltzer, and M. Simons (2004), Updated repeat orbit interferometry package released, *Eos Trans. AGU*, *85*(5), doi:10.1029/2004EO050004.

Sella, G. F., T. H. Dixon, and A. Mao (2002), REVEL: A model for recent plate velocities from space geodesy, *J. Geophys. Res.*, *107*(B4), 2081, doi:10.1029/2000JB000033.

Sigmundsson, F. (2006), *Iceland Geodynamics, Crustal Deformation and Divergent Plate Tectonics*, 209 pp., Springer, Chichester, U. K.

Sigmundsson, F., P. Einarsson, and R. Bilham (1992), Magma chamber deflation recorded by the global positioning system: The Hekla 1991 eruption, *Geophys. Res. Lett.*, *19*, 1483–1486.

Sigmundsson, F., R. Pedersen, K. L. Feigl, E. Sturkell, P. Einarsson, S. Jonsson, K. Agustsson, K. Agustsson, A. Linde, and F. Bretar (2001), Joint interpretation of geodetic data for volcano studies: Evaluation of pre- and co-eruptive deformation for the Hekla 2000 eruption from InSAR, tilt, GPS, and strain data, *Eos Trans. AGU*, *82*(47), Fall Meet. Suppl., Abstract V21E-07.

Soosalu, H., and P. Einarsson (1997), Seismicity around the Hekla and Torfajökull volcanoes, Iceland, during a volcanically quiet period, 1991–1995, *Bull. Volcanol.*, *59*, 36–48, doi:10.1007/s004450050173.

Soosalu, H., and P. Einarsson (2004), Seismic consraints on magma chambers at Hekla and Torfajökull volcanoes, Iceland, *Bull. Volcanol.*, *66*, 276–286, doi:10.1007/s00445-003-0310-1.

Soosalu, H., P. Einarsson, and B. Thorbjarnardóttir (2005), Seismic activity related to the 2000 eruption of the Hekla volcano, Iceland, *Bull. Volcanol.*, *68*, 21–36, doi:10.1007/s00445-005-0417-7.

Sturkell, E., K. Agustsson, A. T. Linde, S. I. Sacks, P. Einarsson, F. Sigmundsson, H. Geirsson, R. Pedersen, and P. La Femina (2005), Geodetic constraints on the magma chamber of the Hekla volcano, Iceland, *Eos Trans. AGU*, *86*(52), Fall Meet. Suppl., Abstract V21D-0636.

Sturkell, E., P. Einarsson, F. Sigmundsson, H. Geirsson, H. Ólafsson, R. Pedersen, E. de Zeeuw-van Dalfsen, A. T. Linde, S. I. Sacks, and R. Stefánsson (2006a), Volcano geodesy and magma dynamics in Iceland, in *The Changing Shapes of Active Volcanoes: Recent Results and Advances in Volcano Geodesy*, edited by M. Poland and A. Newman, *J. Volcanol. Geotherm. Res.*, *150*, 14–34, doi:10.1016/j.jvolgeores.2005.07.010.

Sturkell, E., F. Sigmundsson, and R. Slunga (2006b), 1983-2003 decaying rate of deflation at Askja caldera: Pressure decrease in an extensive magma plumbing system at a spreading plate boundary, *Bull. Volcanol.*, *68*, 727–735, doi:10.1007/s00445-005-0046-1.

Tryggvason, E. (1994), Observed ground deformation at Hekla, Iceland prior to and during the eruption of 1970, 1980-1981 and 1991, *J. Volcanol. Geotherm. Res.*, *61*, 281–291.

Williams, C. A., and G. Wadge (2000), An accurate and efficient method for including the effects of topography in three-dimensional elastic models of ground deformation with applications to radar interferometry, *J. Geophys. Res.*, *105*, 8103–8120.

R. Grapenthin, Geophysical Institute, University of Alaska Fairbanks, Fairbanks, AK 99775, USA.

A. Hooper, Delft Institute of Earth Observation and Space Systems, Delft University of Technology, 2600 AA Delft, Netherlands.

B. G. Ofeigsson and F. Sigmundsson, Nordic Volcanological Center, Institute of Earth Sciences, University of Iceland, Askja, Sturlugata 7, IS-101 Reykjavík, Iceland. (bgo@raunvis.hi.is)

E. Sturkell, Department of Earth Sciences, University of Gothenburg, SE-405 30 Gothenburg, Sweden.